Food Chemistry 202 (2016) 500–506

Contents lists available at ScienceDirect

Food Chemistry

journal homepage: www.elsevier.com/locate/foodchem

Kinetics of conversion of dihydroxyacetone to methylglyoxal in New Zealand mānuka honey: Part III – A model to simulate the conversion

Megan N.C. Grainger [a], Merilyn Manley-Harris [a,*], Joseph R. Lane [a], Richard J. Field [b]

[a] Department of Chemistry, University of Waikato, Private Bag 3105, Hamilton, New Zealand
[b] Department of Chemistry, University of Montana, Missoula, Montana, USA

ARTICLE INFO

Article history:
Received 8 October 2015
Received in revised form 13 January 2016
Accepted 3 February 2016
Available online 4 February 2016

Keywords:
Mānuka honey
Dihydroxyacetone
Methylglyoxal
Conversion
Simulation

ABSTRACT

A kinetic model for the conversion of dihydroxyacetone (DHA) to methylglyoxal (MGO) in honey is proposed; a building block approach was used to create the model. Artificial honeys doped with DHA and individual perturbants were fitted first, then multiple perturbants (alanine, proline and iron, and combinations of these) were fitted before comparing the simulation to real honey samples (doped clover and mānuka honey). The main responses in the prediction model were DHA, MGO, proline, primary amino acids, acidity, 3-phenyllactic acid and 4-methoxyphenyllactic acid. Three temperatures (20, 27 and 37 °C) were studied and the conversion of DHA to MGO was monitored over at least 1 year. Differences in the conversion between clover doped with DHA and mānuka honey were observed. The simulation fitted well for the honeys tested.

1. Introduction

The use of a prediction tool for the formation of methylglyoxyl (MGO) in mānuka honey is becoming increasingly important in the mānuka honey industry because beekeepers, commercial suppliers and exporters are interested in achieving the maximum amount of MGO, and in knowing the time it will take to achieve this, since the higher the MGO concentration, the higher the price for which the honey can be sold. Detailed kinetics data for the conversion of dihydroxyacetone (DHA) to methylglyoxal (MGO) in honey systems is lacking. Most studies have examined the conversion in aqueous systems which differ greatly from the acidic, dehydrating environment of honey (Fedoronko, Temkovic, Mihálov, & Tvaroska, 1980; Fedoroňko & Königstein, 1969; Popoff, Theander, & Westerlund, 1978; Riddle & Lorenz, 1968; Strain & Spoehr, 1930; Weber, 2001). Parts I (Grainger, Manley-Harris, Lane, & Field, 2016a) and II (Grainger, Manley-Harris, Lane, & Field, 2016b) of this series have investigated the conversion of DHA and MGO in mānuka and clover honeys and artificial honeys respectively. Detailed study of the kinetics of transformation in the honeys has allowed assessment of the effect of temperature and time, and the use of perturbants in artificial systems has allowed assessment of the influence of particular compounds on rates of reactions. The several simulations described here assessed the effect of individual perturbants, and groups thereof, and, finally, all influences simultaneously which allowed a realistic model to be created in a stepwise manner.

In an attempt to change the rate at which DHA converts to MGO, time and temperature are the only two variables that can be manipulated, without adulterating the honey. However, individual honeys may show variations in the concentrations of perturbants, which may affect the kinetics.

To build the simulation the following steps have been previously described: (Grainger et al., 2016a, 2016b) (i) reaction pathways were identified using model systems to limit side reactions, (ii) reactions were proposed that might contribute to a model and (iii) some rate constants and activation energies were derived experimentally. In this paper we describe how this information was combined to produce a predictive model for the loss of DHA and gain of MGO in mānuka honey over time at different temperatures. This paper is the first attempt at modelling the conversion of DHA to MGO in a honey matrix and a good fit of the simulation with the experimental data was achieved for the honeys tested.

2. Materials and methods

2.1. Kinetic modelling

A kinetic model was proposed and translated into a mathematical model by converting each reaction step into differential equations. Matlab® 2013a Student Version was used to create the

* Corresponding author.
E-mail address: manleyha@waikato.ac.nz (M. Manley-Harris).

http://dx.doi.org/10.1016/j.foodchem.2016.02.032
0308-8146/

model. Resulting concentrations were compared to experimental data in Minitab® 16 Statistical Software and Microsoft Office Excel 2007.

3. Results and discussion

3.1. Creation of a predictive model at 37 °C

In order to carry out a simulation of a complex set of chemical reactions, all, or at least the most important chemical reactions involving each chemical species, must be considered. Initially, the simplest chemical system was modelled (control system with only DHA), then addition of one perturbant at a time permitted investigation of their influence, followed by addition of two or more perturbing species to the model yielding an increasingly complex system. The simulation was constrained by chemical observations; a model with a set of rate parameters may fit the data, but may not have exact relevance to the system chemically.

It is likely that multiple products were formed from catalysis by, or reaction with, a single perturbant; it was not, however, practically feasible to obtain kinetic data for all of these reactions and some reactions included are assumed to occur based upon relevant literature. The honey matrix is likely to behave differently to the aqueous solutions usually discussed in the literature and individual side products have not yet been identified. It was not necessary to know the exact products that were formed as these are unimportant for the use of this model and rate constants were chosen to reflect the sum of all possible products formed from either DHA or MGO with each perturbant.

The simulation was created using mmol/kg for all species, rather than mg/kg so that the stoichiometry could be easily followed throughout the reactions. A good fit for the simulation was achieved by comparing the simulation and experimental data. To assess the quality of fit, the results from an inter-laboratory comparison program (ILCP) for MGO measurement were used to define an acceptable general deviation (Aleksic & Buckley-Smith, 2013). In this ILCP the standard deviation for mānuka honey ($n = 6$) ranged from 24 to 164 mg/kg (total MGO ranged from 186 to 815 mg/kg MGO). Two laboratories had Z-scores larger than 2; with these two contributions removed, the upper standard deviation was 119 mg/kg (0.32 mmol/kg). In the current study, if the difference between the simulation and experimental data was less than 119 mg/kg it was deemed to be a good fit.

Artificial honey with only DHA added was used as the starting point for the simulation. The intermediate enediol and enolic form of MGO (Strain & Spoehr, 1930) in the conversion were not experimentally measured but were necessary in the simulation to produce the correct DHA vs. time curve. The sum of concentrations of simulated DHA, DHA dimer and enediol were used for comparison to the experimental DHA concentration because all three species are detected as DHA by the analytical method. When analysed by HPLC, the dimer converts to the monomer during sample preparation (2 h in aqueous solution). This is confirmed by the initial theoretical concentration of DHA added to the system matching the reported initial concentration at the start of the reaction. The sum of the simulated concentrations of the enolic form of MGO and MGO were used to compare with the experimental MGO concentration because it is assumed that the enolic form of MGO will rapidly convert to MGO and the reaction from enediol to the enolic form of MGO is irreversible. Initially the model commenced with monomeric DHA but there was an apparent misfit and, when perturbants were added to the model, the simulated conversion occurred much too fast because there was a large supply of monomeric DHA. Incorporation of the DHA dimer into the simulation gave a better fit. Experimentally, an initial fast loss of DHA was observed when proline or alanine were added to the system, indicating that a portion of DHA was present in monomeric form and was free to bind to the amino acid (Grainger et al., 2016b).

Experimentally, the control system (DHA only) did not show a 1:1 conversion of DHA to MGO indicating that a portion of DHA is lost in a side reaction, either by reacting with itself, MGO or sugars. Artificial honey with only MGO added was stable for more than 1 year, confirming that MGO does not react with itself or sugars in the honey matrix. Reaction of DHA with itself and MGO has been reported by Popoff and Theander (1978) and these overall reactions were incorporated into the simulation. The term 'aldol' has been used to depict any product from the reaction of two DHA. This is an irreversible pathway and accounts for the loss of DHA in the control sample. If this is set as a reversible equation in the model all of the DHA will eventually end up as MGO (a sink), but this in not seen experimentally. Since these individual pathways and the concentration of the products are unknown, all possible side reactions with a perturbant were incorporated as a single pathway. The rate constants were chosen accordingly to encompass the effect of the various pathways and to provide the best fit for the data.

The conversion of DHA to MGO in the control system was much slower than the conversion reported in real honey matrices (Grainger et al., 2016a) or aqueous systems. The honey environment is extremely dehydrating and DHA is likely to predominantly exist as the unreactive dimer, not the monomer. In aqueous solution, the rate determining step is likely to be the formation of the enediol; however, in the honey environment the dissociation of the DHA dimer to monomeric DHA is likely to be the rate determining step for the entire scheme. The small amount of monomeric DHA present in the system introduces competition between different species for the limited supply of DHA. The control system does not have proton donating species which can catalyse the conversion of the dimer to the monomer and thus accelerate the conversion of DHA to MGO. Incorporation of the dimer in the simulation ties up a large proportion of the DHA and renders it unavailable; this fits the experimental data well. Further evidence for the dimer was observed in systems perturbed by amino acids; systems with individual amino acids had an initial fast loss of DHA, but systems with two amino acids did not have a cumulative loss of DHA indicating that only a limited portion of DHA is present as the monomer (Grainger et al., 2016b). Thus a large proportion of DHA cannot be quickly depleted by a perturbing species since most DHA is tied up as the dimer. A ratio of 75:25 dimer: monomer was chosen to best fit the experimental work. The simulation follows the same trends that DHA and MGO exhibit (first-order plot of MGO deviating from linearity at later times in the reaction) for the various experimental systems observed. The rate constants defined for the control sample were used as the base rate for all subsequent models with added perturbants.

The system perturbed by alanine (as a proxy for all primary amino acids) had an initial fast reaction most likely due to alanine binding to DHA. This is likely to be a reversible reaction such as occurs in the first stages of the Maillard Reaction, for example formation of a Schiff base (discussed in Part II (Grainger et al., 2016b)); this reaction temporarily ties up a portion of alanine so that it reduces the catalytic ability of alanine. Reversible binding of DHA and alanine was incorporated into the model and slowed down the formation of MGO. In the experimental systems, the rate constant for loss of DHA after rapid initial loss was the same as for the control system, but the rate constant for MGO appearance was larger and the efficiency of the reaction was higher, indicating that alanine either prevents DHA from entering a side reaction or recovers it from one and allows it to convert to MGO. Initially in the simulation, the conversion of two DHA to the aldol was reversible, but as mentioned above this allowed MGO to become a sink, which was not seen experimentally and too much DHA was lost compared to the experimental data for this system. Therefore it was

proposed that alanine could provide an alternative pathway from the aldol to form two MGO. This may be a multistep reaction, but has been encompassed in one step in the simulation. The loss of DHA vs. time and gain of MGO vs. time plots for the simulated data fitted the experimental data well and the efficiency of the simulated reaction also matched the experimental data. Details on the reaction between the aldol and alanine are currently unknown. Popoff and Theander (1978) reported various cyclic products formed from DHA reacting with itself or MGO. Formation of the aldol is likely to occur through multiple steps and may include one or more of the structures proposed by Popoff and Theander (1978). The alanine may donate a proton to an early intermediate before cyclisation occurs, allowing it to split and form MGO. It is probable that only a portion of the aldol can convert to MGO and this has been reflected in the rate constant. Addition of an irreversible reaction between alanine and MGO helped to control the amount of DHA and MGO present in the system, but did not fit the experimental results since a model system with MGO and alanine displayed no change in MGO concentration over 500 days. Without this reaction in the simulation too much DHA was lost due to its reaction with alanine. Therefore a reaction between alanine and an unknown compound A was used to remove a portion of alanine from the system. Alanine is less reactive than other amino acids but will form Maillard products (Iglesias et al., 2006; Sanz, del Castillo, Corzo, & Olano, 2003) and is likely to react with acyclic sugars. A small lag phase in MGO production in seen in the simulated data while the aldol concentration builds up. This does not correspond to the experimental results for this system.

Alanine was used in a higher concentration in the model system compared to concentrations of total primary amino acids in real honey. Therefore in real honey primary amino acids will not make a large contribution to the formation of MGO. Furthermore, not all amino acids will behave in the same manner; for example, Iglesias, de Lorenzo, Polo, Martín-Álvarez, and Pueyo (2004) and Sanz et al. (2003) have both reported that alanine was not as reactive in honey compared to other amino acids. The rate constant for the reaction with acylic sugars of lysine, with two amino groups, is expected to be much larger than for alanine, with only one. Lysine is more readily lost in food matrices compared to other amino acids due to its free ε-amino group; this substantial loss occurs before the formation of brown pigments (Saltmarch & Labuza, 1982). Furthermore, lysine is reported as the most reactive amino acid tested when reacted with DHA at pH 4 and 5 in aqueous solutions (Kawashima, Itoh, & Chibata, 1980). In part I of this series individual amino acids showed strong correlations with the rate constant for DHA loss (Grainger et al., 2016a). The concentration of total primary amino acids between different mānuka honeys is not expected to vary by orders of magnitude. Therefore once a set of rate constants have been chosen for the reactions involving amino acids they should work for a large number of samples and thus individual amino acid concentration. Consequently, individual amino acid concentrations would not have to be determined for each honey analysed in the prediction model.

The experimental model system perturbed by proline demonstrated an initial fast loss of DHA (corresponding on a molar basis to the amount of proline added) indicating binding of the DHA by proline; this was followed by a slower reaction that had a rate constant which was a factor of two smaller than the control system. This may be due to the limited H^+ available for dissociation of the dimer, due to DHA and proline binding reversibly. Furthermore, a system with MGO and proline showed a loss in MGO over time (Grainger et al., 2016b).

Addition to the simulation of equations for the reversible reaction between DHA and proline did not fit the experimental data either for DHA or for MGO because the slow loss of DHA could not be simulated and insufficient MGO was formed; this suggests a small enhancement of the reaction from proline that is not reflected in the overall rate constant for MGO appearance. While an equation for this improved the MGO fit, the DHA simulation still did not fit the experimental data. Eventually the model was refined for a system perturbed by both proline and alanine. The experimental rate constant for DHA loss in systems with proline and one or more other perturbants was not slower than the control system due presumably to the ability of the other perturbants to dissociate the dimer. A competing reaction between proline and the other perturbant for the free DHA would mean not as much DHA could initially bind to proline, hence some proline would be available to catalyse a side reaction of MGO. MGO appearance was too slow due to a loss of MGO at later times when rate constants for alanine and proline were simply added together. This was accounted for by a catalytic conversion of MGO into a side product by proline (Fig. 1). This equation was not required in the system perturbed by only proline because not enough MGO was formed to notice the loss at longer times. The system perturbed by both proline and alanine was modelled with good accuracy confirming these assumptions.

Experimentally, iron (II) did not catalyse side reactions of either DHA or MGO. Addition to the simulation of equations for reversible binding of DHA and iron (II) and the iron (II) catalysed conversion of DHA to MGO were able to fit the simulation to the experimental data. However, high levels of iron are not observed in real honey, hence this equation will not have a large effect in real honey systems.

Rate constants for alanine and iron, and for proline and iron were added together and matched the experimental data indicating that there was no synergy between the pairs of perturbants. When all three sets of rate constants were added together the simulated data fitted the experimental data well.

3.2. Comparison of prediction model with real honey

Experimental data for DHA-doped clover honey and mānuka honey stored at 37 °C were compared to the simulation; the simulated DHA concentrations were only slightly too slow, but there was an apparent misfit for MGO – formation was too slow and the simulated data was linear, not curved like the experimental data. The primary amino acid content in real honey is much lower than in the model systems, hence it is unable to convert the aldol to MGO. This indicates that other compounds are responsible for this role in real honey that were not accounted for in the model systems. Grainger et al. (2016a) identified that total acidity and phenolic compounds were correlated to the disappearance of DHA. It was assumed that in clover honey, the total acidity is largely made up of gluconic acid. An equation for the catalytic conversion of DHA to MGO by organic acids (measured as total acidity) and loss of organic acids over time were added and gave a better fit for clover honeys doped with DHA. Although phenolic acids were not specifically investigated in model systems during the experimental phase, they were an obvious factor to consider in the model since certain phenolic acids are found in large quantity in mānuka honeys (Oelschlaegel et al., 2012; Stephens et al., 2010; Tan, Holland, Wilkins, & Molan, 1988; Wilkins, Lu, & Molan, 1993) and thus must contribute to the total acidity. The most likely role for these is as proton donors to facilitate the production of monomeric DHA from the dimer and they were added to the model accordingly. For mānuka honey, conversion of DHA to MGO catalysed by phenolic acid was added to the simulation. The total acidity of mānuka honey is some 50% higher than for clover honey (31.91 ± 5.61 meq/kg compared to 21.75 ± 4.73 meq/kg (Grainger et al., 2016a)). This is undoubtedly due to the phenolic acids; any other organic acid present would not be expected to produce an outcome that differed from clover. The total concentration of

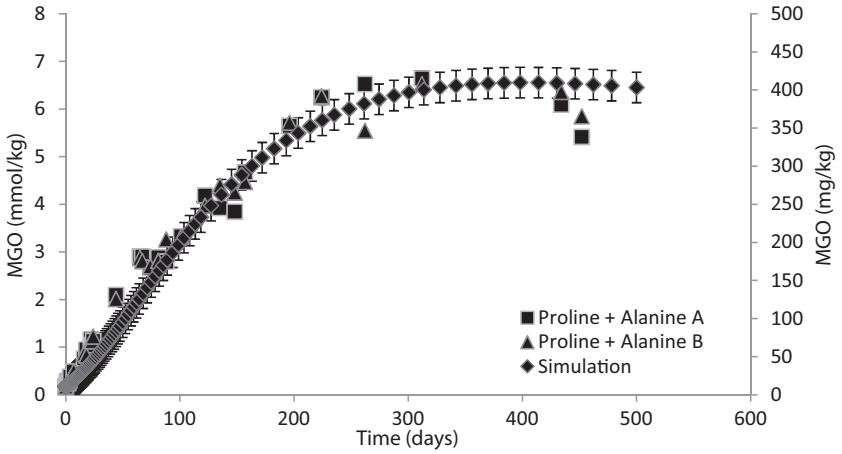

Fig. 1. Experimental data (circles and squares) and simulated data (triangles) for gain of MGO in an artificial honey system perturbed by alanine and proline (two replicates). An equation for the removal of MGO catalysed by proline was added into the model to help simulate the curve at later times in the reaction. Error bars (0.32 mmol/kg, 119 mg/kg) relate to the standard deviation reported in the 2013 ILCP. The simulated data fits the experimental data well.

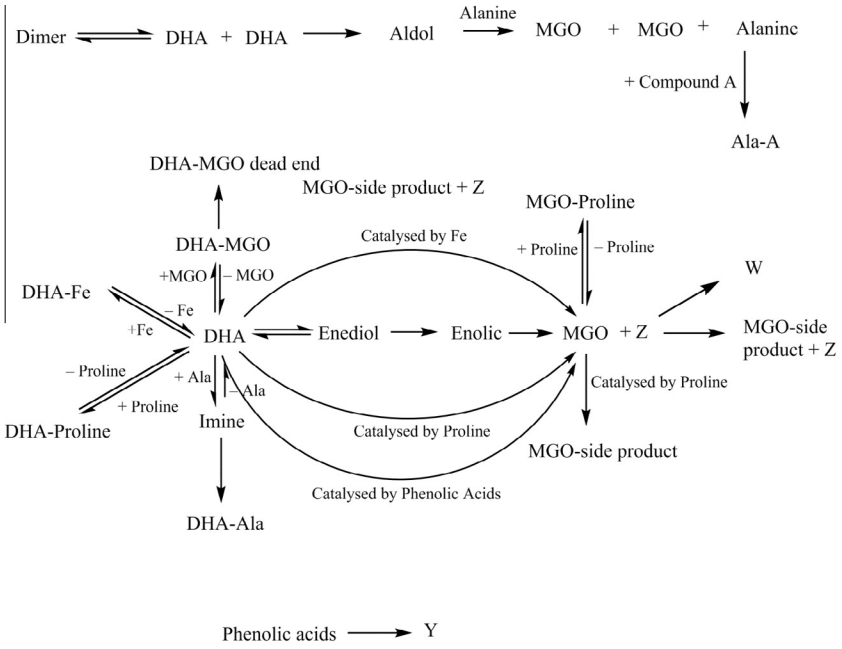

Fig. 2. Final model including proposed pathways for the conversion of DHA to MGO and their side reactions as established from the model systems (Grainger, Manley-Harris, Lane, & Field, 2016b) and real honey systems (Grainger et al., 2016a). Alterations of this model compared to the initial model includes conversion of DHA to MGO from catalysis of phenolic acids, removal of phenolic acids by an unknown compound "Y", removal of MGO by an unknown compound "Z" and the removal of "Z" to "W".

phenyllactic acid and 4-methoxyphenyllactic acid was used in the model. This gave a very good fit for DHA and also brought the MGO curve closer to the experimental data early in the course of maturation, but too much MGO was gained later in the reaction. Addition of syringic acid and 2-methoxybenzoic acid to the total phenolic acids did not change the fit due to their low concentrations in the samples. The removal of phenolic acids (by conversion to a compound arbitrarily named Y) was also required as a way of slowing down the reaction over time. However, even with this equation added, the simulated MGO concentration did not decline in the same way as the experimental data at prolonged times at 37 °C; note that this decline was not observed at lower temperatures or in the clover matrix. The compounds responsible for removal of MGO at later times in mānuka honey are currently unknown, so were collectively called Z in the simulation. MGO is a very reactive compound and most likely form a range of Maillard-type compounds at this stage of the simulation; α-oxoaldehydes, such as MGO, are 20,000-fold more reactive than glucose in glycation processes, therefore they bypass the requirement for a fructosamine precursor in the formation of advanced glycation end products (AGEs) (Thornalley, 1996) and hence are likely to be reacting in the honey matrix. The starting concentration of Z had to be altered for each sample so that the simulation fitted the experimental data, indicating that the concentration of compounds responsible varies between samples and could possibly be regional, as observed for the phenolic acids. Phenolic acids were tried in the place of Z, but did not fit the model, suggesting that either the model needs refining or phenolic acids are not solely responsible for the loss of MGO at later times. Furthermore, reversible and irreversible reactions between MGO and Z were used in an attempt to fit the simulation to the experimental data, but these did not strengthen the prediction. However, the removal

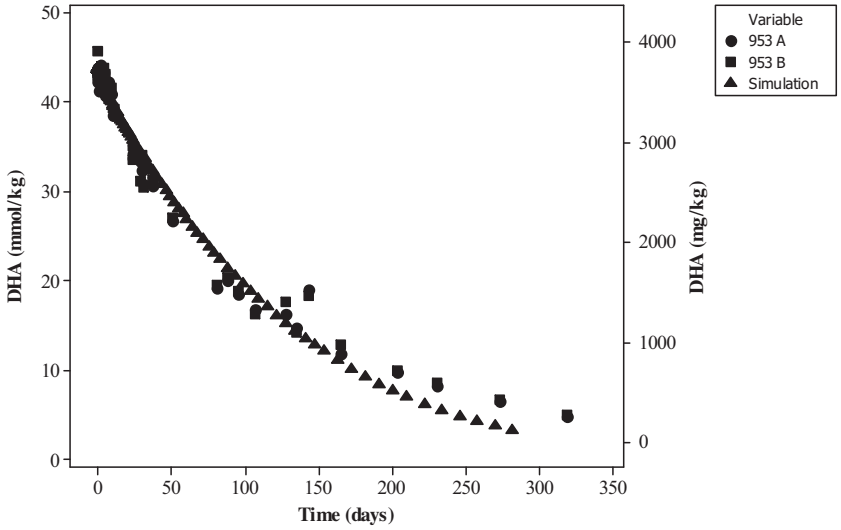

Fig. 3. Experimental (circles and squares) and simulated (triangles) data for loss of DHA in mānuka honey 953 at 37 °C. The simulated data fits the experimental data well.

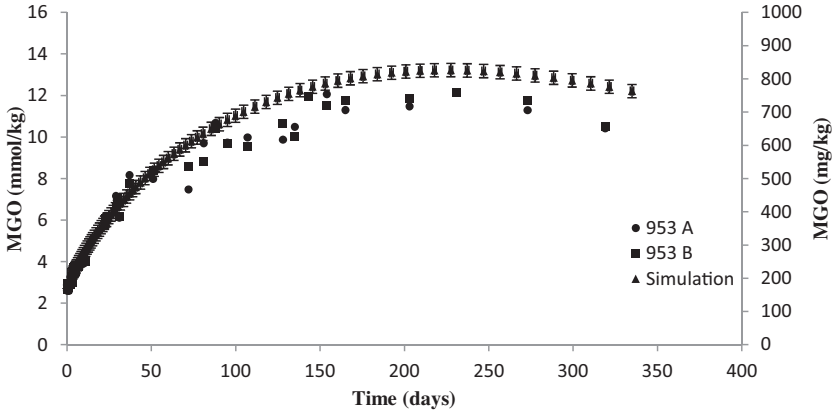

Fig. 4. Experimental (circles and squares) and simulated (triangles) data for gain of MGO in mānuka honey 953 at 37 °C. The error bars are set at ±0.32 mmol/kg (119 mg/kg) as determined by the standard deviation in the 2013 ILCP. The simulated data fits the experimental data initially, however, slightly too much MGO is formed at later times in the simulated data.

of compound Z to arbitrary compound W, which encompasses all possible compounds formed, was required for the simulation to fit the experimental data so that excess MGO was not removed. The final model for prediction of the conversion of DHA to MGO in mānuka honey is shown in Fig. 2. The model is depicted in three unconnected schemes to reduce the complexity which arises from the stoichiometric differences associated with the DHA dimer; however, it must be remembered that all reactions are connected by DHA. The phenolic acids converting to a further product are also shown separately.

It is possible that the model could also have been adapted so that phenolic acids dissociate the aldol in a similar manner to the alanine (catalysis); however, no model systems containing phenolic acids were examined, hence it is unknown whether or not phenolic acids recover DHA from an otherwise dead end pathway. A plot for the disappearance of DHA vs. time for both experimental and simulated data is shown in Fig. 3, which has good accuracy. A plot for the formation of MGO vs. time for both experimental and simulated data is shown in Fig. 4. The initial formation of MGO is within the error chosen from the ILCP, but slightly too much MGO is formed in the simulation at later times, indicating further work is required to find compounds responsible for the removal of MGO at later times at 37 °C.

3.3. Influence of species – robustness

The influence of each main species within the simulation was examined by altering the initial concentration of one species over the range at which it would naturally occur while holding the initial concentration of all other species the same. As the concentration of alanine is increased, more MGO is ultimately formed due to the ability of alanine to release DHA from the aldol species. Fig. 5 shows variation in concentration of MGO over time for different alanine concentrations. The non-peroxide activity (NPA), which is related to MGO, (Adams et al., 2008, 2009) is shown on the secondary axis to give a commercially relevant impression of the change in NPA when the model is stressed. In contrast, as the concentration of proline increases, the amount of MGO formed decreases due to the catalytic role of proline in removing MGO as a side product (Fig. 6). Variation in neither compound affected the amount of DHA that was lost in the simulation.

The concentration of phenolic acids influenced the concentration of both DHA and MGO because the simulation incorporates the conversion of DHA to MGO catalysed by phenolic acids acting directly on the DHA, rather than the aldol. As the phenolic acid concentration increased, the amount of DHA lost and MGO gained also increased and this effect was significant. The higher the

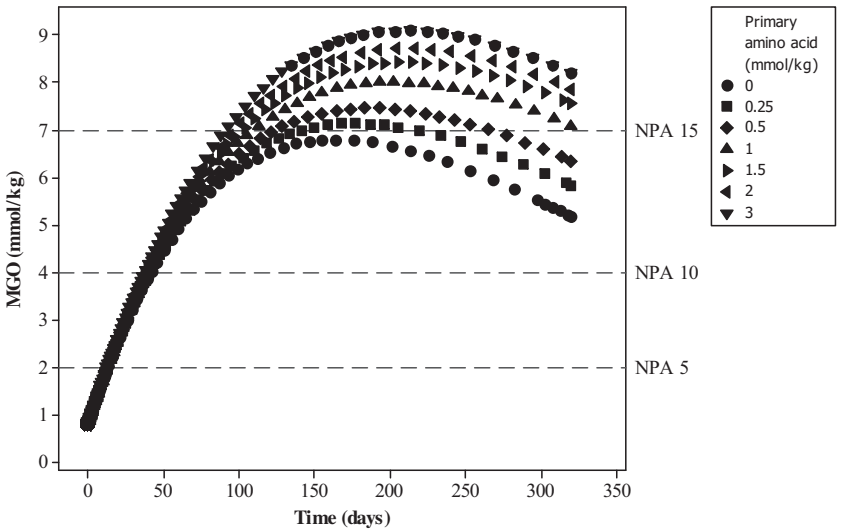

Fig. 5. Simulated gain of MGO with various starting concentrations of primary amino acid (0–3 mmol/kg). The simulation included total phenolic acids and Z (6 and 5 mmol/kg respectively). Non-peroxide activity (NPA) has been inserted on the secondary axis to give a visual estimate of the change when the model is stressed.

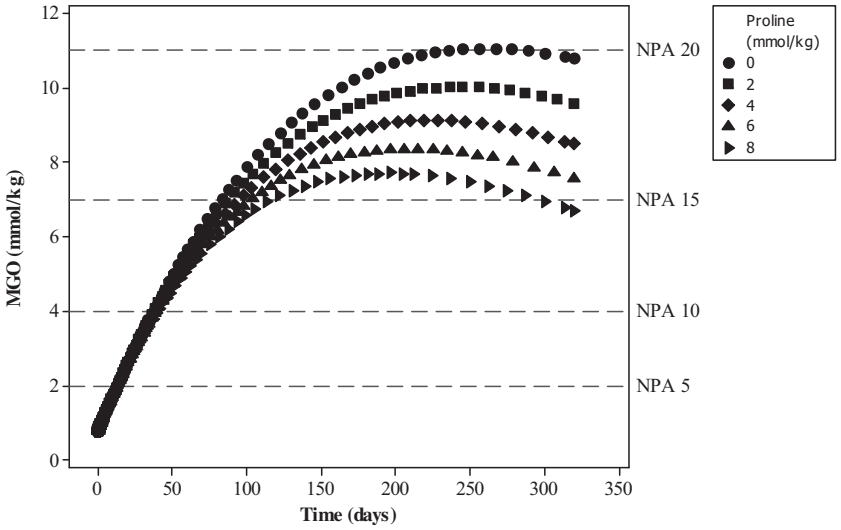

Fig. 6. Simulated gain of MGO with various starting concentrations of proline (0–920 mg/kg). The simulation included total phenolic acids and Z (6 and 5 mmol/kg respectively). Non-peroxide activity (NPA) has been inserted on the secondary axis to give a visual estimate of the change when the model is stressed.

concentration of compound Z, the more MGO that was lost at later times.

3.4. Simulation at 20 and 27 °C

The rate constants for the simulation at 37 °C were compared to the model systems at 20 and 27 °C in order to adjust the rates. Not all of the reactions were affected by altering the temperature. At 27 °C rate constants for the equilibrium between the DHA dimer and monomer, reaction of DHA and MGO with side products and reactions involving proline, the side reaction of phenolic acids, the catalysis of the aldol to MGO by alanine and the reaction of MGO with Z were all reduced by a factor of 5. The rate constant for the catalytic reaction of DHA to MGO by phenolic acids was only reduced by a factor of 3. Reactions containing alanine were unaffected by the change in temperature. The simulation fitted experimental data for real honeys with these new rate constants. At 20 °C, most rate constants were the same as for systems at 27 °C; the rate constants for the conversion of DHA to the enediol and the reversible reaction between DHA and MGO were lowered in the control equations. The rate constants for the equations involving proline were the same as for the reaction at 27 °C. The rate constants for the equations involving alanine were reduced further. The simulation fits well at the lower temperatures because the loss of MGO at later times is not prominent after one year of storage.

4. Conclusion

This is the first time that a predictive model for the conversion of DHA to MGO at various temperatures has been reported in the literature. It is a starting point for understanding the factors that influence the fate of both DHA and MGO within the honey matrix at different temperatures. At temperatures of 20 °C and 27 °C the model provided a good fit to the data but at 37 °C the loss of MGO that occurs at extended times resulted in a slight over-estimation of MGO in the simulation.

Funding sources

Megan N.C. Grainger was supported by The University of Waikato Doctoral Scholarship, Fulbright Travel Award, Claude McCarthy Travel Scholarship, New Zealand Federation of Graduate Women Charitable Trust Waikato Branch Award and Shirtcliffe Fellowship.

Acknowledgements

The authors wish to thank Steens Honey Ltd and Kevin Gibbs for donation of honey and the latter for participating in storage trials.

References

Adams, C. J., Boult, C. H., Deadman, B. J., Farr, J. M., Grainger, M. N. C., Manley-Harris, M., et al. (2009). Corrigendum to "Isolation by HPLC and characterization of the bioactive fraction of New Zealand mānuka (*Leptospermum scoparium*) honey". *Carbohydrate Research, 344*(18). 2609–2609 [Carbohydr. Res. 343 (2008) 651].

Adams, C. J., Boult, C. H., Deadman, B. J., Farr, J. M., Grainger, M. N. C., Manley-Harris, M., & Snow, M. J. (2008). Isolation by HPLC and characterisation of the bioactive fraction of New Zealand mānuka (*Leptospermum scoparium*) honey. *Carbohydrate Research, 343*(4), 651–659.

Aleksic, G., & Buckley-Smith, M. (2013). Inter-laboratory comparison programme: Antibacterial activity in manuka honey – October 2013. In (p. 11). Hamilton, New Zealand: Global Proficiency.

Fedoroňko, M., & Königstein, J. (1969). Kinetics of mutual isomerisation of trioses and their dehydration to methylglyoxal. *Collection Czechoslovak Chemical Communications, 34*, 3881–3894.

Fedoronko, M., Temkovic, P., Mihálov, V., & Tvaroska, I. (1980). Kinetics and mechanism of the acid-catalyzed reactions of methylated trioses. *Carbohydrate Research, 87*(1), 51–62.

Grainger, M. N. C., Manley-Harris, M., Lane, J. R., & Field, R. J. (2016a). Kinetics of conversion of dihydroxyacetone to methylglyoxal in New Zealand mānuka honey: Part I – Honey systems. *Food Chemistry, 202*, 484–491.

Grainger, M. N. C., Manley-Harris, M., Lane, J. R., & Field, R. J. (2016b). Kinetics of conversion of dihydroxyacetone to methylglyoxal in New Zealand mānuka honey: Part II – Model systems. *Food Chemistry, 202*, 492–499.

Iglesias, M. T., de Lorenzo, C., Polo, M. d. C., Martín-Álvarez, P. J., & Pueyo, E. (2004). Usefulness of amino acid composition to discriminate between honeydew and floral honeys. Application to honeys from a small geographic area. *Journal of Agricultural and Food Chemistry, 52*(1), 84–89.

Iglesias, M. T., Martín-Álvarez, P. J., Polo, M. C., de Lorenzo, C., González, M., & Pueyo, E. (2006). Changes in the free amino acid contents of honeys during storage at ambient temperature. *Journal of Agricultural and Food Chemistry, 54*(24), 9099–9104.

Kawashima, K., Itoh, H., & Chibata, I. (1980). Nonenzymatic browning reactions of dihydroxyacetone with amino acids or their esters. *Agricultural and Biological Chemistry, 44*(7), 1595–1599.

Oelschlaegel, S., Gruner, M., Wang, P.-N., Boettcher, A., Koelling-Speer, I., & Speer, K. (2012). Classification and characterization of mānuka honeys based on phenolic compounds and methylglyoxal. *Journal of Agricultural and Food Chemistry, 60*, 7229–7237.

Popoff, T., Theander, O., & Westerlund, E. (1978). Formation of aromatic compounds from carbohydrates. VI. Reactions of dihydroxyacetone in slightly acidic, aqueous solution. *Acta Chemica Scandinavica B, 32*(1), 1–7.

Riddle, V., & Lorenz, F. W. (1968). Nonenzymic, polyvalent anion-catalyzed formation of methylglyoxal as an explanation of its presence in physiological systems. *Journal of Biological Chemistry, 243*(10), 2718–2724.

Saltmarch, M., & Labuza, T. P. (1982). Nonenzymatic browning via the Maillard reaction in foods. *Diabetes, 31*(3), 29–36.

Sanz, M. L., del Castillo, M. D., Corzo, N., & Olano, A. (2003). 2-Furoylmethyl amino acids and hydroxymethylfurfural as indicators of honey quality. *Journal of Agricultural and Food Chemistry, 51*(15), 4278–4283.

Stephens, J. M., Schlothauer, R. C., Morris, B. D., Yang, D., Fearnley, L., Greenwood, D. R., & Loomes, K. M. (2010). Phenolic compounds and methylglyoxal in some New Zealand mānuka and kanuka honeys. *Food Chemistry, 120*(1), 78–86.

Strain, H. H., & Spoehr, H. A. (1930). The effect of amines on the conversion of trioses into methylglyoxal. *The Journal of Biological Chemistry, 89*, 527–534.

Tan, S. T., Holland, P. T., Wilkins, A. L., & Molan, P. C. (1988). Extractives from New Zealand honeys. 1. White clover, mānuka and kanuka unifloral honeys. *Journal of Agricultural and Food Chemistry, 36*(3), 453–460.

Thornalley, P. J. (1996). Pharmacology of methylglyoxal: formation, modification of proteins and nucleic acids, and enzymatic detoxification – A role in pathogenesis and antiproliferative chemotherapy. *General Pharmacology: The Vascular System, 27*(4), 565–573.

Weber, A. (2001). The sugar model: Catalytic flow reactor dynamics of pyruvaldehyde synthesis from triose catalysed by poly-L-lysine contained in a dialyzer. *Origins of Life and Evolution of the Biosphere, 31*, 231–240.

Wilkins, A. L., Lu, Y., & Molan, P. (1993). Extractable organic substances from New Zealand unifloral manuka (*Leptospermum scoparium*) honeys. *Journal of Apicultural Research, 32*(1), 3–9.